RAD Conference Proceedings, vol. 6, pp. 43–48, 2022
ISSN 2466-4626 (online) | DOI: 10.21175/RadProc.2022.08
www.rad-proceedings.org

RADIATION SHIELDING PROPERTIES OF 5% HDPE/BORON COMPOSITES

Selcen Uzun Duran[1,3*], Ümit Alver[2], Brunilda Mucogllava[3], Bilge Demirköz[3], Fatih Özkalayci[4]

[1]Karadeniz Technical University, Vocational School of Health Sciences, Program of Medical Imaging Techniques, Trabzon, Turkey
[2]Karadeniz Technical University, Metallurgical and Materials Engineering, Trabzon, Turkey
[3]IVME-R, The Research and Application Center for Space and Accelerator Technologies, Middle East Technical University, Ankara, Turkey
[4]Karadeniz Technical University, Central Research Laboratory, Trabzon, Turkey

Abstract. *In this study, the material was formed by adding 5 wt% boron into high density polyethylene material to be used in applications containing neutrons. This paper discusses the neutron and gamma rays shielding characteristics of HDPE-based composite materials containing 5% HDPE/colemanite (HDPE/C), 5% HDPE/ulexite (HDPE/U), and 5% HDPE/B2O3 (HDPE/B) by weight additives were fabricated. The characterizations of these shielding materials were determined using scanning electron microscopy (SEM), x-ray diffraction (XRD). The Total macroscopic cross-section of each composite was determined using a ^{239}Pu-Be (α, n) neutron source.*

Keywords: *neutron shield, borated polyethylene, HDPE, 5wt% boron minerals*

1. INTRODUCTION

Neutron radiation can be used in various applications like; neutron radiography studies, activation analysis, medical radiotherapy, 3D imaging technology and more [1-2]. Although neutrons are ionizing type of radiation, their interaction with cells and tissues in the human body can often cause radiological activation and permanent damage [3]. The radiation weighting factor of neutrons of about 1 MeV is higher than that of photons, charged particles such as electrons and protons, and is almost equal to the weighting factor of alpha radiation [4]. Subsequently, radiation protection safety measures are a priority for facilities working with neutrons.

A good neutron radiation shielding material is composed of light elements such as hydrogen (H) and carbon (C) to lower neutron energy, and combination of elements that have high neutron absorption cross section (σ_{abs}) such as boron (B), lithium (Li) and cadmium (Cd) for neutron capture. Therefore, hydrogen-rich polymers can be used to thermalize neutrons (at kinetic energy of 0.025 eV 20 °C), neutrons whose energy drops to the thermal neutron energy level are then captured and absorbed by compounds that contains boron. The higher the number of suspended neutrons, the better the shield's neutron attenuation efficiency [5].

The most used polymers for shielding neutrons are hydrogen rich polymer materials like polyethylene, paraffin, epoxy, polyamide, etc. The most effective one among these is HDPE ([C2H4]n) which has a high hydrogen content (14% hydrogen by weight), relatively high density (0.96 g/cm^3), exceptional strength to density ratio, and ability to withstand high temperatures (120 °C) [6]. Polyethylene is the most popular material for neutron shielding; however, it is not preferred to be used in reactors because the heat-resistant temperature is low. It is mostly used in accelerators, research laboratories, hospitals (linac, oncology, etc.). Highly efficient thermal neutron capturing additives like boron carbide (B4C), boron nitride (BN) and boron oxide (B2O3) are mixed into the HDPE base. Among the commercially available shielding materials, there are; B_2O_3/paraffin [7-8], B_2O_3/natural rubber (NR) [9], and nano-B_4C /high density polyethylene (HDPE) [10] composites. Nevertheless, B_4C and BN are expensive. Therefore, focus of current research is on cost-effective, natural B_2O_3 containing minerals such as colemanite, ulexite, and borax.

Colemanite ($Ca_2B_6O_{11}.5H_2O$) and ulexite ($NaCaB_5O_9.8H_2O$) are among the most important of the 200 known borate minerals [11-13]. They are used in a variety of applications [14], including radiation protection, for which there is an extensive literature [15-21]. Colemanite has a structure that is monoclinic, its specific weight is 2.52 g/cm^2, and it contains up to 50.8% B_2O_3 (15.78% boron) by weight [22-23]. It is generally used in glass production, high-tech ceramics [24] and as a neutron absorbing material in radiation shields [24-32]. Ulexite has a specific weight of 1.96 g/cm^2, contains up to 43% B_2O_3 (13.34% boron) by weight, and is a common sodium-calcium borate hydrate mineral which Turkey has a lot of, used to produce raw boric acid, boron oxides and sodium perborate materials [33].

In the simulation study, it was observed that the neutron absorption rate of HDPE with 5% boron

* selcenduran@ktu.edu.tr

mineral added was better than HDPE, and this rate did not change significantly as the additive increased [34]. In this study, composite materials that are based on HPDE, containing 5% colemanite, 5% ulexite and 5% B_2O_3 by weight additives were produced. These shielding materials were studied by using scanning electron microscopy (SEM), x-ray diffraction (XRD) techniques. The subtraction section of each composite was determined using a ^{239}Pu-Be (α,n) neutron source.

2. MATERIALS AND METHODS

2.1. Materials

In this study HDPE was chosen as the matrix materials and colemanite, ulexite, glassy boron oxide particles were used as filler materials. The commercial HDPE polymer with a trade name Petilen YY 1860(O) used in this study was in the form of pellets and obtained by PETKIM, Petrochemical Holding Inc. (Turkey). Its melt index is 7.5 g/10 min at 190 °C, density at room temperature is 0.96 gr/cm^3 and and Vicat softening temperature is 126 °C.

Colemanite ($Ca_2B_6O_{11}{\cdot}5H_2O$), ulexite ($NaCaB_5O_9{\cdot}8H_2O$) minerals and glassy boron oxide (B_2O_3) compound were supplied by ETI-MADEN (Turkey) and were used as received.

2.2. Sample preparation

Colemanite, ulexite and B_2O_3 were dried first in a vacuum oven at 80 °C for 36 h. Then HDPE/colemanite (HDPE-5C), HDPE/ulexite(HDPE-5U), and HDPE/B_2O_3 (HDPE-5B), composites with 5 weight percent were fabricated using a co-rotating twin screw extruder (L/D: 40). The temperature profile from feed zone to die zone was set at 190, 195, 200, 210 and 215 °C while the rotation speed of the screw was fixed at 120 rpm. The composites were extruded in the form of strands through a die into a distilled water bath at room temperature and granulated into pellets. Since the obtained pellets were moist, they were dried in an oven at 80 °C for 24 h. This extrusion process was repeated 2 times to improve the dispersivity of filler particles in the HDPE matrix.

Figure 1. Photograph of doped composite materials produced in the form of a 5 mm thick and 7.5 cm diameter disc

After pelletizing, HDPE/colemanite, HDPE/ulexite, and HDPE/B_2O_3 composites were dried in a vacuum oven at 80 °C for 36 h and these dried composites were converted into test samples in an injection molding machine for neutron absorption testing. The samples for neutron absorption test were obtained in form of a circular disc with 7.5 cm of diameter and 5 mm of thickness. The produced discs are shown in Figure 1.

2.3. Characterization

Chemical analyses of the samples were carried out using a Perkin Elmer model AA 400 atomic absorption spectrometer (AAS) and the results are given in Table 1. The density of the composites is determined by Archimedes method. In order to determine the structure, the HDPE/colemanite, HDPE/ulexite, and HDPE/B2O3 composites were characterized using PANalytical X'Pert3 Pro X-Ray Diffractometer (XRD) using Cu-Ka radiation (λ =1.541874 Å) in a range of $5 \le 2\theta \le 75$ with scan speed of 30/min. A Zeiss Evo LS10 scanning electron microscope (SEM) was used to observe the dispersion of fillers inside HDPE. The cryogenically fractured surface of the samples was used for morphology observation and each specimen was coated with gold to reduce the charge resulting from electron bombardment.

Table 1. Chemical content of colemanite, ulexite and B2O3

Component	Colemanite	Ulexite	B2O3
	Composition (%)		
B_2O_3	39.2	35.7	78.2
CaO	28.7	22.4	-
H_2O	22	35	17
Na_2O	1.9	2.7	-
MgO	2.1	2.5	-
Others	6.1	1.7	4.8

2.4. Neutron absorption analysis

Neutron shielding tests were carried out using a Nuclear-Chicago NH_3 Howitzer with a 5 Curie ^{239}Pu-Be (α,n) isotopic neutron source. The neutron strength, which is utilised for the normalization of flux values, equals $1.6{\times}10^6$ $s^{-1}Ci^{-1}$. The energy spectrum corresponds to the interval between 0 and 10.5 MeV, where the mean energy (E_{mean}) is equal to 4.24 MeV [35].

The source, 2.59 cm in diameter and 11.2 cm in height, is found at the center of the Howitzer, surrounded by a paraffin base with a 28.5 cm radius, encapsulated with a 0.3 cm thick aluminum drum. An empty 3 cm in radius channel connects the source to the Howitzer's exit. A plexiglass rod is connected to the source from the top and is used to parallel it to the test channel during irradiation testing. Figure 2 shows the test setup. Neutrons exit through the test channel indicated with '2' where the prepared shielding samples, indicated with '3', are positioned. Sample to source distance is 29 cm, whereas sample to detector distance is 21 cm. Radiation shielding material blocks are used to stop neutrons and the accompanying gamma rays from exiting the test area [35].

Figure 2. Pu-Be tests setup as seen from above with its main components numbered 1 to 5 (a) and the exit channel seen from the prospective of the neutron detector. The detector's main body is found under the shielding aligned with the exit channel

For each of the fabricated samples, the neutron removal cross-section was determined using the following relationship:

$$\Sigma = \frac{\ln(I/I_0)}{x} \qquad (1)$$

where Σ is the macroscopic removal cross-section, I0 is the incident neutron intensity, I is the transmitted neutron intensity and x is the sample thickness [28].

Neutron intensities, given in counts per second (cps), were measured using a Polimaster PM1401K neutron detector with an energy sensitivity range of 0.025 eV to 14 MeV. Once the detector's position was fixed, I0 measurements were taken. Then, the fabricated disk samples were placed at the exit one by one to measure the I's for each of the three mixtures for sample thicknesses up to 4 cm.

3. Results and Discussion

3.1. SEM and XRD analysis of HDPE composites

The SEM images of cryogenically fractured surfaces of HDPE composite materials filled with 5wt% colemanite, 5wt% ulexite, and 5wt% B_2O_3 are shown in Figure 3 (a), (b), (c), respectively.

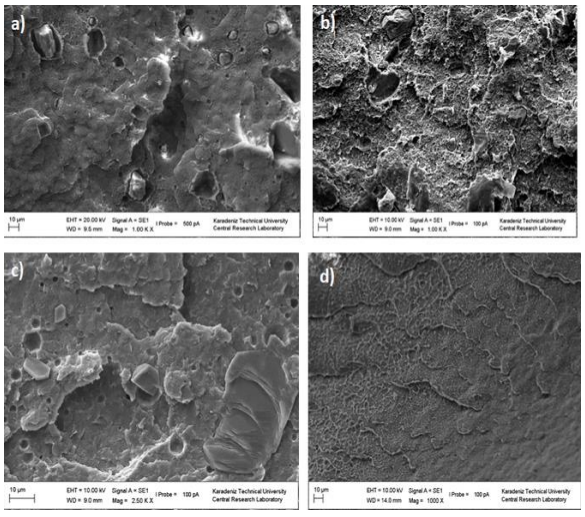

Figure 3. The SEM images for 5wt% colemanite (a), 5wt% ulexite (b), 5wt% B2O3 (c) filled HDPE, and (d) pure HDPE

The cryogenically fractured surface of the samples was used for morphology observation. SEM images show that the colemanite, ulexite and B2O3 additives were homogeneously dispersed in the HDPE polymer. But, as seen in Fig. 3, the fillers are debonded and pulled-out from the HDPE matrix. Besides, some voids were seen in composites. These indicate that the filler particles are adhered poorly in the HDPE matrix.

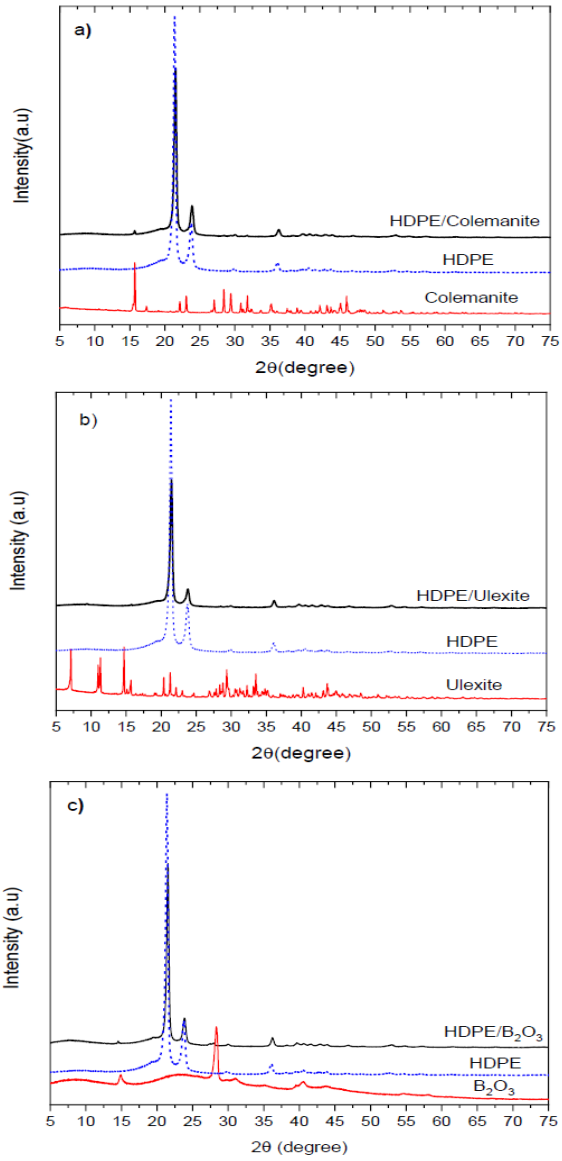

Figure 4. The XRD pattern for (a) 5wt% colemanite, (b) 5wt% ulexite and (c) 5wt% B2O3 filled HDPE composites

As seen in Figure 4, the filler particles are dispersed homogeneously and are adhered poorly in the HDPE matrix. The XRD patterns for HDPE/colemanite, HDPE/ulexite, and HDPE/B_2O_3 composites are illustrated in Figure 4a-c. As illustrated in the XRD spectra, the HDPE has a characteristic maximum intensity peak at $2\theta = 21.47^{o}$, In addition to the strong HDPE peak, some week reflection peaks belonging to colemanite, ulexite and B_2O_3 particles are seen.

3.2. Density and Porosity of HDPE composites

Experimental and theoretical densities of the HDPE composites are listed in Table 2. Experimental densities were obtained by using Archimedes' principle. The theoretical density of composites in terms of weight fraction were computed using equation

$$\rho_c=1/[(w_f/\rho_f)+(w_m/\rho_m)] \qquad (2)$$

where, w and ρ represent the weight fraction and density respectively. The suffix f, m, and c stand for the filler, matrix, and the composite materials respectively [36]. In calculation, theoretical densities of colemanite, ulexite and B_2O_3 were taken as 2.42 g/cm^3, 2.13 g/cm^3 and 2.17 g/cm^3, respectively.

Table 2. Experimental and theoretical values of HDPE, HDPE-5C, HDPE-5U and HDPE-5B composites

Materials	Experimental Density (g/cm^3)	Theoretical Density (g/cm^3)
HDPE	0.958±0.01	0.960
HDPE-5C	0.981 ± 0.01	1.055
HDPE-5U	1.001±0.02	1.046
HDPE-5B	1.014±0.01	1.048

From Table 2, it is clearly seen that theoretical density values are higher than experimental density values. This difference indicates that HDPE composite materials contain some voids and pores in structure. The reason for this, might be release of the crystal water in colemanite, ulexite and B_2O_3 when the composites are extruded.

3.3. Neutron absorption test

In this study, the neutron absorption properties of high-density polyethylene materials containing 5% boron by weight (ulexite-colemanite-B_2O_3) were determined by using a ^{239}Pu-Be neutron source. Figure 5-a gives the neutron transmission I/I_o (transmitted radiation intensity/initial radiation intensity, I/I_o results for the 5% by weight of the borated polymer (B-PE) mixtures compared to pure HDPE.

The relationship between neutron transmission ratio and sample thickness of the 5% by weight borated polymer mixtures is compared to pure HDPE and their corresponding Σtot.

The highest neutron macroscopic cross section was boron oxide, then colemanite, and lastly ulexite. But all of them have better neutron absorption cross section than pure HDPE.

The total macroscopic cross-section (Σ) is the cross section used in the calculation of the attenuation of neutrons. The total macroscopic cross sections (Σ) for ^{239}Pu-Be neutron source was derived from Figure 5-b by utilizing Eq. (1). The neutron attenuation feature was discussed taking into account the total neutron attenuation. Total macroscopic cross-sections (Σ) data for neutrons presented in Table 3.

As seen Table 3, All Boron mineral filled HDPE composites have higher neutron absorption rate than pure HDPE material. In addition, among the composites, the best neutron absorption rate is HDPE-5B composites. As seen in Table 3, the materials with the highest macroscopic cross section are HDPE-5B, HDPE-5C, HDPE-5U, respectively. All three minerals can be used as shielding material in neutron-containing applications.

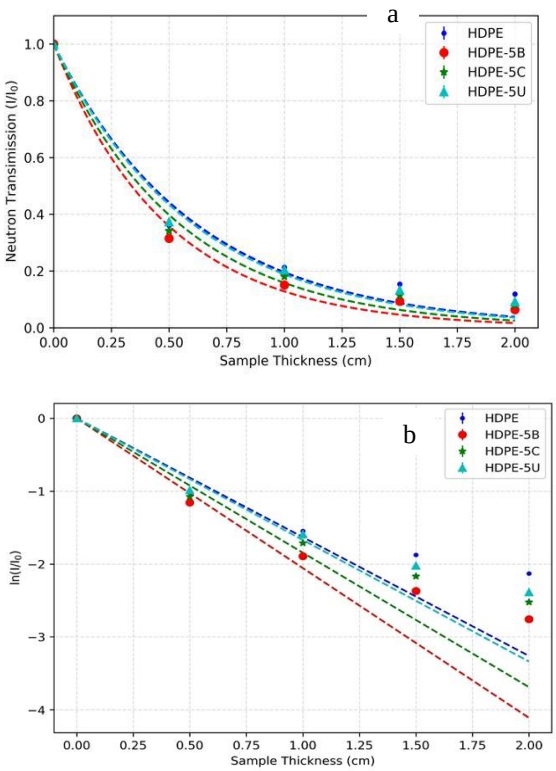

Figure 5-a. The relationship between neutron transmission ratio and sample thickness of the 5% by weight borated polymer mixtures compared to pure HDPE and their corresponding Σtot. Figure 5-b. ln(I/I0) as a function of the thickness of the studied materials.

Table 3. Total macroscopic cross-sections (Σ) of of HDPE, HDPE-5C, HDPE-5U and HDPE-5B composites.

Materials	Σ_{tot} (cm^{-1})
HDPE	1.63±0.04
HDPE-5B	2.05±0.03
HDPE-5C	1.84±0.03
HDPE-5U	1.67±0.02

4. Conclusion

In this study, a shielding material was produced for applications containing neutrons by adding 5% boron minerals to high density polyethylene material. The neutron attenuation properties of the produced materials were investigated.

Among the three borate additives used, B_2O_3 showed the best neutron absorption performance, followed closely by colemanite.

The neutron absorption rates of these three materials produced are much better than pure high density polyethylene material. These three materials can be used as neutron absorbing materials. Here, ease

of production and place of use come to the fore. It is suitable for use in places such as hospitals, neutron therapy, laboratories and accelerators rather than environments that reach high temperatures.

Acknowledgements: *The paper is a part of the research done within the TUBITAK-1505 Project (project no. 5190039). The authors would like to thank Eti Mine Works General Management for providing boron ores.*

REFERENCES

1. K. Nedunchezhian, N. Aswath, M. Thiruppathy, T. Sarumathi, "Boron neutron capture therapy – A literature review," *Journal of Clinical and Diagnostic Research,* vol. 10, no. 12, pp. ZE01–ZE04, Dec. 2016. https://doi.org/10.7860/JCDR/2016/19890.9024
2. A. Tengattini, N. Lenoir, E. Andò, G. Viggiani, "Neutron imaging for geomechanics: A review," *Geomechanics for Energy and the Environment*, vol. 27, article no. 100206, Sep. 2021. https://doi.org/10.1016/j.gete.2020.100206
3. E. B. Podgoršak, "Interactions of Neutrons with Matter," in *Radiation Physics for Medical Physicists. Biological and Medical Physics, Biomedical Engineering*, Berlin-Heidelberg, Germany: Springer, 2009, ch. 9, pp. 429–449. https://doi.org/10.1007/978-3-642-00875-7_9
4. "The 2007 Recommendations of the International Commission on Radiological Protection. ICRP publication 103," *Ann. ICRP*, vol. 37, no. 2–4, pp. 1–332, 2007. https://doi.org/10.1016/j.icrp.2007.10.003
5. S. Th. Abdulrahman, Z. Ahmad, S. Thomas, A. A. Rahman, "Chapter 1 – Introduction to neutron-shielding materials," in *Micro and Nanostructured Composite Materials for Neutron Shielding Applications, Woodhead Publishing Series in Composites Science and Engineering*, S. Th. Abdulrahman, S. Thomas, Z. Ahmad, Eds., Sawston, UK: Woodhead Publishing, 2020, ch. 1, pp. 1–23. https://doi.org/10.1016/B978-0-12-819459-1.00001-5
6. V. More, Z. Alsayed, M. S. Badawi, A. A. Thabet, P. P. Pawar, "Polymeric composite materials for radiation shielding: a review," *Environmental Chemistry Letters,* vol. 19, pp. 2057–2090, Feb. 2021. https://doi.org/10.1007/s10311-021-01189-9
7. P.A. Zyla et al., "Review of Particle Physics," *Progress of Theoretical and Experimental Physics,* vol. 2020, no. 8, pp. 612–617, Aug. 2020. https://doi.org/10.1093/ptep/ptaa104
8. D. Toyen, K. Saenboonruang, "Development of paraffin and paraffin/bitumen composites with additions of B_2O_3 for thermal neutron shielding applications," *Journal of Nuclear Science and Technology*, vol. 54, no. 8, pp. 871–877, May 2017. https://doi.org/10.1080/00223131.2017.1323688
9. K. Ninyong, E. Wimolmala, N. Sombatsompop, K. Saenboonruang, "Potential use of NR and wood/NR composites as thermal neutron shielding materials," *Polymer Testing*, vol. 59, pp. 336–343, May 2017. https://doi.org/10.1016/j.polymertesting.2017.02.020
10. J. Kim, B. C. Lee, Y. R. Uhm, W. H. Miller, "Enhancement of thermal neutron attenuation of nano-B_4C, -BN dispersed neutron shielding polymer nanocomposites," *Journal of Nuclear Materials*, vol. 453, no. 1–3, pp. 48–53. Oct. 2014. https://doi.org/10.1016/j.jnucmat.2014.06.026
11. K. Okuno, M. Kawai, H. Yamada, "Development of Novel Neutron Shielding Concrete," *Nuclear Technology,* vol. 168, no. 2, pp. 545–552, 2009. https://doi.org/10.13182/NT09-A9241
12. M. Gönen, E. Nyankson, R. B. Gupta., "Boric acid production from colemanite together with ex situ CO_2 sequestration," *Industrial & Engineering Chemistry Research*, vol. 55, no. 17, pp. 5116–5124, 2016. https://doi.org/10.1021/acs.iecr.6b00378
13. G. Celik, T. Depci, A. M. Kılıc, "New lightweight colemanite-added perlite brick and comparison of its physico mechanical properties with other commercial lightweight materials," *Construction and Building Materials*, vol. 62, pp. 59–66, Jul. 2014. https://doi.org/10.1016/j.conbuildmat.2014.03.031
14. O. M. Kalfa, Z. Üstündağ, İ. Özkırım, Y. K. Kadıoğlu, "Analysis of tincal ore waste by energy dispersive X-ray fluorescence (EDXRF) Technique," *Journal of Quantitative Spectroscopy and Radiative Transfer*, vol. 103, no. 2, pp. 424–427, Jan. 2007. https://doi.org/10.1016/j.jqsrt.2006.02.059
15. F. Demir, A. Un, "Radiation transmission of colemanite, tincalconite and ulexite for 6 and 18 MV X-rays by using linear accelerator," *Applied Radiation and Isotopes*, vol. 72, pp. 1–5, Feb. 2013. https://doi.org/10.1016/j.apradiso.2012.09.020
16. T. Korkut et al., "Investigation of neutron shielding properties depending on number of boron atoms for colemanite, ulexite and tincal ores by experiments and FLUKA Monte Carlo simulations," *Applied Radiation and Isotopes,* vol. 70, no. 1, pp. 341–345, Jan. 2012. https://doi.org/10.1016/j.apradiso.2011.09.006
17. H. Binici, O. Aksogan, A. H. Sevinc, A. Kucukonder, "Mechanical and radioactivity shielding performances of mortars made with colemanite, barite, ground basaltic pumice and ground blast furnace slag," *Construction and Building Materials*, vol. 50, pp. 177–183, Jan. 2014. https://doi.org/10.1016/j.conbuildmat.2013.09.033
18. G. Cosansu, C. Cogun, "An investigation on use of colemanite powder as abrasive in abrasive waterjet cutting (AWJC)," *Journal of Mechanical Science and Technology,* vol. 26, pp. 2371–2380, Aug. 2012. https://doi.org/10.1007/s12206-012-0619-9
19. C. Kaynak, N. A. Isitman, "Synergistic fire retardancy of colemanite, a natural hydrated calcium borate, in high-impact polystyrene containing brominated epoxy and antimony oxide," *Polymer Degradation and Stability*, vol. 96, no. 5, pp. 798–807, May 2011. https://doi.org/10.1016/j.polymdegradstab.2011.02.011
20. N. A. Isitman, C. Kaynak, "Effect of partial substitution of aluminum hydroxide with colemanite in fire retarded low-density polyethylene," *Journal of Fire Sciences*, vol. 31, no. 1, pp. 73–84, 2013. https://doi.org/10.1177/0734904112454835
21. R. Bagheri, S. P. Shirmardi, R. Adeli, "Study on Gamma-Ray Shielding Characteristics of Lead Oxide, Barite, and Boron Ores Using MCNP-4C Monte Carlo Code and Experimental Data," *Journal of Testing and Evaluation,* vol. 45, no. 6, pp. 2259–2266, 2017. https://doi.org/10.1520/JTE20160284
22. S. Kalay, Z. Yilmaz, M. Çulha, "Synthesis of boron nitride nanotubes from unprocessed colemanite," *Beilstein Journal of Nanotechnology*, vol. 4, pp. 843–851, 2013. https://doi.org/10.3762/bjnano.4.95
23. Ö. Sallı Bideci, "The effect of high temperature on lightweight concretes produced with colemanite coated pumice aggregates," *Construction and Building Materials,* vol. 113, pp. 631–640, Jun. 2016. https://doi.org/10.1016/j.conbuildmat.2016.03.113
24. T. Uysal, H. S. Mutlu, M. Erdemoğlu, "Effects of mechanical activation of colemanite ($Ca_2B_6O_{11}·5H_2O$) on its thermal transformations," *International*

Journal of Mineral Processing, vol. 151, pp. 51–58, Jun. 2016. https://doi.org/10.1016/j.minpro.2016.04.006

25. F. Demir, "Determination of mass attenuation coefficients of some boron ores at 59.54keV by using scintillation detector," *Applied Radiation and Isotopes*, vol. 68, no. 1, pp. 175–179, Jan. 2010. https://doi.org/10.1016/j.apradiso.2009.09.003
26. K. Okuno, "Neutron shielding material based on colemanite and epoxy resin," *Radiation Protection Dosimetry*, vol. 115, no. 1–4, pp. 258–261, Dec. 2005. https://doi.org/10.1093/rpd/nci154
27. T. Korkut et al., "Neutron dose transmission measurements for several new concrete samples including colemanite," *Annals of Nuclear Energy,* vol. 37, no. 7, pp. 996–998, Jul. 2010. https://doi.org/10.1016/j.anucene.2010.04.005
28. S. M. Malkapur et al., "Neutron radiation shielding properties of polymer incorporated self-compacting concrete mixes," *Applied Radiation and Isotopes*, vol. 125, pp. 86–93, Jul. 2017. https://doi.org/10.1016/j.apradiso.2017.03.029
29. A. Mesbahi, G. Alizadeh, G. Seyed-Oskoee, A.-A. Azarpeyvand, "A new barite–colemanite concrete with lower neutron production in radiation therapy bunkers," *Annals of Nuclear Energy,* vol. 51, pp. 107–111, Jan. 2013. https://doi.org/10.1016/j.anucene.2012.07.039
30. T. Korkut et al., "Investigation of neutron shielding properties depending on number of boron atoms for colemanite, ulexite and tincal ores by experiments and FLUKA Monte Carlo simulations," *Applied Radiation and Isotopes,* vol. 70, no. 1, pp. 341–345, Jan. 2012. https://doi.org/10.1016/j.apradiso.2011.09.006
31. E. M. Derun, A. S. Kipcak, "Characterization of some boron minerals against neutron shielding and 12 year performance of neutron permeability," *Journal of Radioanalytical and Nuclear Chemistry*, vol. 292, pp. 871–878, 2012. https://doi.org/10.1007/s10967-011-1528-6
32. T. Bel, C. Arslan, N. Baydogan, "Radiation shielding properties of poly (methyl methacrylate) / colemanite composite for the use in mixed irradiation fields of neutrons and gamma rays," *Materials Chemistry and Physics,* vol. 221, pp. 58–67, Jan. 2019. https://doi.org/10.1016/j.matchemphys.2018.09.014
33. A. Albarodi, P. Uslu Kiçeci, S. Uzun Duran, B. Demirköz, "Monte-Carlo (MC) analysis of borated materials for neutron shielding applications," *Eurasian Journal of Science Engineering and Technology*, vol. 3, no. 2, pp. 63–70, Dec. 2022. https://doi.org/10.55696/ejset.1102371
34. N. Demirkıran, A. Künkül, "Dissolution kinetics of ulexite in perchloric acid solutions," *International Journal of Mineral Processing*, vol. 83, no. 1–2, pp. 76–80, Jul. 2007. https://doi.org/10.1016/j.minpro.2007.04.007
35. A. I. Topuz , I. A. Reyhancan, "Neutronic Analysis of a Nuclear-Chicago NH3 Neutron Howitzer," *eprint arXiv:1806.05255*, Jun. 2018. https://doi.org/10.48550/arXiv.1806.05255
36. M. E. Mahmoud et al., "Fabrication, characterization and gamma rays shielding properties of nano and micro lead oxide-dispersed-high density polyethylene composites," *Radiation Physics and Chemistry*, vol. 145, pp. 160–173, Apr. 2018. https://doi.org/10.1016/j.radphyschem.2017.10.017